The submitted manuscript has been authored by a contractor of the U. S. Government under contract No. W-31-109-ENG-38. Accordingly, the U. S. Government retains a nonexclusive, royalty-free license to publish or reproduce the published form of this contribution, or allow others to do so, for U. S. Government purposes.

FERMILAB
MAY 29 1996
LIBRARY

ANL-HEP-CP-96-22
For the Proceedings of the
Adriatico Research Conference on
"Trends in Collider Spin Physics"
Trieste, Italy, 5-8 December 1995

ANL-HEP-CP-96-22

Fermilab Library
0 1160 0042730 4

COLLIDER SPIN PHYSICS AT RHIC AND STAR*

A. YOKOSAWA
High Energy Physics Division
Argonne National Laboratory, Argonne, Illinois 60439 USA

Abstract

The first polarized collider, where we collide 250-GeV/c beams of 70% polarized protons at high luminosity, is under construction. This will allow a determination of the nucleon spin-dependent structure functions over a large range in x, and a collection of sufficient W and Z events to investigate extremely interesting spin-related phenomena.

For these measurements, two major RHIC detectors will be used simultaneously whose functions are complimentary. Expected event rates given in this paper are for the STAR detector.

1. Introduction

We begin by discussing the status of a polarized collider at the Relativistic Heavy Ion Collider (RHIC). In August 1991, a partial snake experiment at AGS was approved by the Brookhaven Program Advisory Committee (PAC). Then in August 1992 proposals by the RHIC Spin Collaboration (RSC), STAR/Spin, and PHENIX/Spin were submitted to the PAC. In October 1993, full approval of the proposals was granted by the BNL PAC. Our major objectives are on gluon and sea-quark spin dependent structure function measurements, parity-violating asymmetry measurements, and transversity measurements. The measurements involve jets, direct-γ, $W^{\pm}$ and Z° production. In April 1994, successful proton acceleration in the AGS with a partial snake was achieved, and further work will be continued. In September 1995 the Memorandum of Understanding for the RIKEN (the Institute of Physical and Chemical Research, Japan)/BNL Collaboration on the Spin Physics Program at RHIC was signed. Thus, RIKEN will be responsible for the spin-related facilities at RHIC.

Proposed spin experiments at RHIC are to explore QCD in a new way, and allow us to make the first direct measurement on the proton structure functions. Quarks and leptons may consist of more fundamental constituents and have a composite structure. The fascinating feature of composite models of quarks and leptons is that the interaction generally violate parity. By measuring parity violating asymmetries, the composite structure may be studied.

* This work supported by the U.S. Department of Energy, Division of High Energy Physics, Contract W-31-109-ENG-38.

2. Present State of the Nucleon Spin

Using deep inelastic scattering experiments, internal structure in the proton was found, the x distributions of the quark were measured, and the spin distribution of the quarks was investigated.

However, deep inelastic scattering can not fully explain the spin of the proton. It also can not cover the right kinematic range to be described in the RHIC spin measurements.

We summarized here activities of spin measurements at various laboratories:

HERMES at HERA --	is not high enough Q^2 in ep, and uses polarized gas target in pp.
HERA with polarized protons and polarized electrons --	not suited for gluon, sea-quark spin, and $h_1(x)$ studies.
SLAC capabilities --	lie between HERMES and polarized HERA.
Fermilab --	No approval for spin physics.
Son of SMC --	Very hard way to study gluon spin, and not yet approved.
RHIC --	In the right energy range, and the relevant x region, to make a full investigation of the nucleon spin.

3. Polarized Proton Collisions at BNL

Figure 1 shows the Brookhaven hadron facility complex, which includes the AGS booster, the AGS, and RHIC. The solenoidal partial snake is installed in a 3-meter straight section in the AGS. The RHIC spin project will install two snakes per ring with four spin rotators per detector for achieving helicity-spin experiments.

4. High Energy Spin Physics at RHIC

We present physics issues, the estimates of the acceptances of STAR, and expected event rates for various reactions.

The integrated luminosities used are:

$Ldt = 8 \cdot 10^{38}\ cm^{-2} at\ 500\ GeV = 800\ pb^{-1}$, $Ldt = 3 \cdot 2^{38}\ cm^{-2} at\ 200\ GeV = 320\ pb^{-1}$,

which mean 100 days of running $\left(4 \cdot 10^{6}\ \text{sec. } 50\%\ efficiency\right)$.

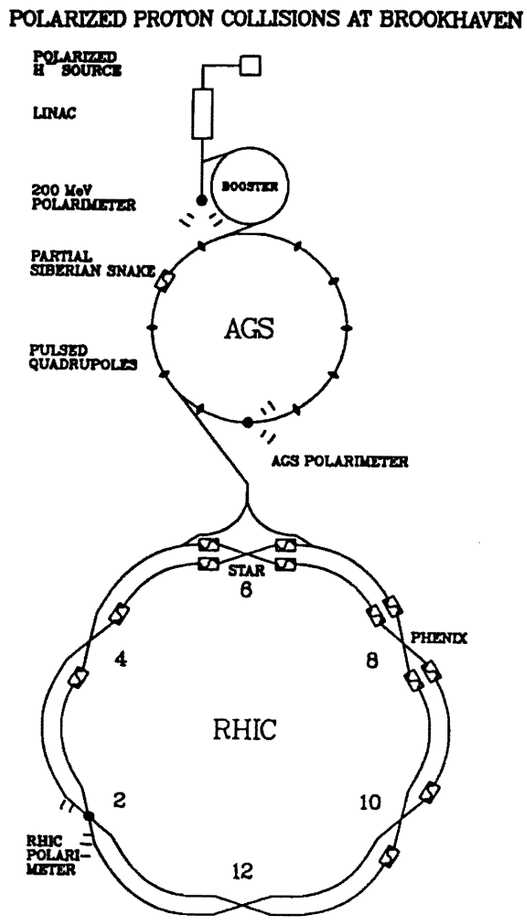

Figure 1 AGS Booster, AGS, RHIC

The RHIC polarized collider allows us to explore QCD in a new way, and opens challenging opportunities for QCD studies.

The proton spin consists of:

$$1/2 \sum \Delta q + \Delta G + < Iz > = 1/2$$

Our proposed measurements are to determine sea-quark polarization, $\Delta\bar{u}(x)$ and $\Delta\bar{d}(x)$, and gluon polarization $\Delta G(x)$. We are also to determine one of the fundamental proton structure functions $(f_1, g_1, \text{and } h_1)$.

Let us consider the hadronic reaction, pp $\rightarrow$ (hadron or gauge boson) + X. When both initial protons are longitudinally polarized, we measure an observable A_{LL} defined as:

$$A_{LL} = \left(1/P^2\right)\left(N^{++} - N^{+-}\right)/\left(N^{++} + N^{+-}\right).$$

If one QCD subprocess is dominant:

$$A_{LL} \sim P_a \cdot P_b \cdot \hat{a}_{LL}(a + b \rightarrow c + d),$$

where $\hat{a}_{LL}$ are helicity asymmetries for various subprocesses obtained from perturbative QCD.

4.1 Measurements with Barrel EMC and Shower Maximum Detector

The STAR barrel EM calorimeter is a lead-scintillator sampling calorimeter. It is located inside the aluminum coil of the STAR solenoid and covers $|\eta| \leq 1.0$ and 2π in azimuth, thus matching the acceptance for full TPC tracking. At $\eta \sim 0$, the amount of material in front of the EMC is ~ 0.5 radiation lengths (X_o). The inner radius is 2.20 meters, and the overall length is 6.20 meters.

A detector, with fine spatial resolution, will be placed at a depth of approximately five X_o, near the location of the maximum number of shower electrons for photons of 3-5 GeV, to allow for the detection of direct photons. It will reject background photons emanating from decaying π^o mesons having $p_T \leq 20$ GeV/c, by examining the transverse shower profile at this depth. The radial space allotted for this device is 25 mm[1].

4.1.1 Jet Production at 200 GeV

Several QCD subprocesses contribution to the cross section for jet production:

a) gluon-gluon scattering at low p_T
b) gluon-quark scattering at medium p_T (above ~ 20 GeV/c), and
c) quark-quark elastic scattering at high p_T.

At low p_T:

$$A_{LL} = \left[\Delta G(x_1)/G(x_1)\right] \bullet \left[\Delta G(x_2)/G(x_2)\right] \bullet \hat{a}_{LL}(gg \rightarrow gg).$$

The $\hat{a}_{LL}$ is expected to be large, $\hat{a}_{LL} = 0.8$ at 90°.

The EM component of jets are detected with the EMC, and the charged particles using the TPC. The ability of the STAR EMC to trigger efficiently on events containing hard parton scatters, while rejecting minimum bias events, is important for high-luminosity events.

Jet rapidity: $|\eta| > 0.3$ corresponding to $0.05 < x < 0.3$.

Sizable rates for jets occur for p_T up to 50 GeV/c

4.1.2 Di-Jet Production at 200 GeV

The advantage over the single jet is the kinematic constraint on the momentum fractions, x_i of the two partons.

Jet + Jet Events		
p_T	$\|\eta\|$	N_{pair}
≥ 10	≤ 0.3	$1 \bullet 10^8$
≥ 20	≤ 0.3	$3 \bullet 10^6$

4.1.3 Direct-γ Production at 200 GeV

Direct photons are produced through the $q\bar{q}$ annihilation subprocess and the quark-gluon Compton subprocess, ($qg \rightarrow \gamma q$). The Compton process is the dominant one in pp interactions. Then,

$$A_{LL} = [\Delta u(x_1)/u(x_1)] \bullet [\Delta G(x_2)/G(x_2)] \bullet \hat{a}_{LL}(qg \rightarrow \gamma q),$$

where $\Delta u(x)/u(x) = [u_+(x) - u_-(x)]/[u_+(x) + u_-(x)]$, $\Delta u(x)$ being the helicity distribution of the quark, and $\Delta G(x)/G(x) = [G_+(x) - G_-(x)]/[G_+(x) + G_-(x)]$, where $\Delta G(x)$ is the helicity distribution carried by gluon fields. For example, $\Delta u(x)/u(x) \approx 0.4$ at $x_q = 0.2$ (from EMC - SMC), $\hat{a}_{LL} = 0.6$ at 90° scattering. Then we have $A_{LL} = 0.2 \times \Delta G/G$ and $\delta(\Delta G/G) = 5 \times \delta A_{LL}$. The estimated δA_{LL} at $\sqrt{s} = 200$ GeV for $p_T = 10$ to 20 GeV, $\Delta y \pm 1$, is

$$\delta A_{LL} \sim \pm 0.006 \text{ and } \delta(\Delta G/G) \sim \pm 0.03.$$

4.1.4 Direct-γ + Jet

For the p_T acceptance of 10 to 20 GeV, x_1 and x_2 vary from 0.1 to 0.2 at $\sqrt{s}$ = 200 GeV. The expected number of events is 9,000 corresponding to

$$\delta A_{LL} \sim \pm 0.03$$

4.1.5 Measurements of the Sea-Quark Helicity Distribution in the Drell-Yan Process

The Drell-Yan process appears to be one way to determine the polarization of sea quarks. The $q\bar{q}$ annihilation into a vector boson gives a large asymmetry at the partonic level, and selects sea antiquarks along with valence quarks.

The asymmetry A_{LL} for Drell-Yan in pp collisions is related to the sea-quark helicity distribution:

$$A_{LL} = \hat{a}_{LL} \frac{\Sigma_i e_i^2 \left[\Delta q_i(x_1)\, \Delta\bar{q}_i(x_2) + \Delta q_i(x_2)\, \Delta\bar{q}_i(x_1)\right]}{\Sigma_i e_i^2 \left[q_i(x_1)\, \bar{q}_i(x_2) + q_i(x_2)\, \bar{q}_i(x_1)\right]},$$

where $x_1 - x_2 = x_F$, $x_1\, x_2 = M^2/s$, and $\hat{a}_{LL} = -1$.

4.1.6 $W^{\pm}$ and Z° Production at 500 GeV

i) Parity-Violating Asymmetry

W bosons are predicted to be produced by a parity-violating mechanism, using standard model couplings. The observable $A_L(PV)$ is defined as, $A_L = (N^- - N^+)/(N^- + N^+)$, where -(+) are minus (plus) helicity. For W^+,

$$A_L = \frac{\Delta u(x_1)\, \bar{d}\,(x_2) - \left(u \leftrightarrow \bar{d}\right)}{u(x_1)\, \bar{d}\,(x_2) + \bar{d}\,(x_1)\, u(x_2)}.$$

When the helicities of both beams are the same, we define another observable as:

$$A_{LL}^{PV}(y) = \frac{\left[\Delta u(x_1)\, \bar{d}(x_2) - \Delta\bar{d}(x_2)\, u(x_1)\right] - \left(u \leftrightarrow \bar{d}\right)}{\left[u(x_1)\, \bar{d}(x_2) - \Delta(x_1)\, \Delta\bar{d}(x_2)\right] + \left(u \leftrightarrow \bar{d}\right)}.$$

For y = 0, $A_L^{W^+} = 1/2\ (\Delta u/u - \Delta\bar{d}/d)$ and $A_L^{W^-} = 1/2\ (\Delta d/d - \Delta\bar{u}/u)$. The results of predictions[2] for $W^{\pm}$ production are shown in Fig. 2 with polarized sea quarks[3] and $\Delta\bar{u} = \Delta\bar{d}$. In the case of W^- production, one observes a drastic difference between the cases $\Delta\bar{u} \neq 0$ and $\Delta\bar{u} = 0$. Figure 3 shows how well we can determine $\Delta\bar{d}/\bar{d}$.

Figure 2

The parity violating asymmetry A_{LL}^{PV} vs. y for W+ and W- production at $\sqrt{s}$ = 500 GeV. Solid lines correspond to non-zero sea quark polarizations where as dashed lines correspond to $\Delta\bar{u} = \Delta\bar{d} = 0$.

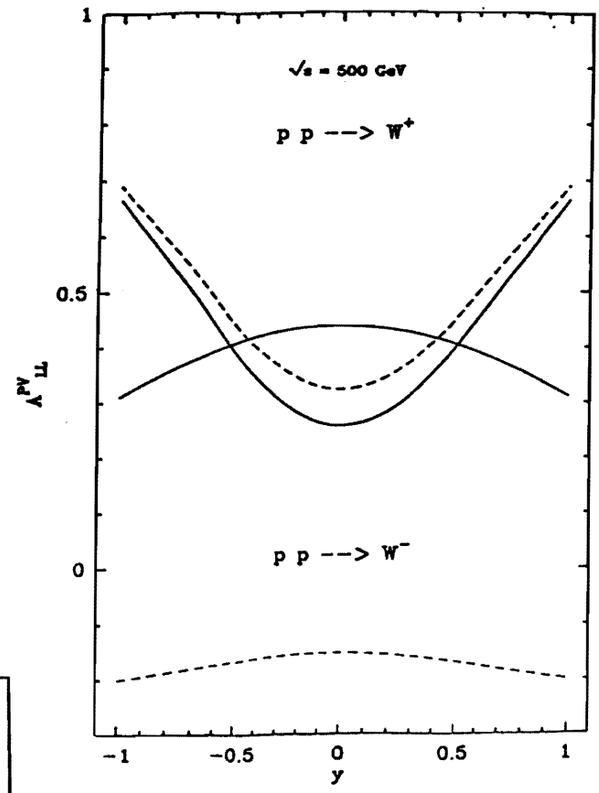

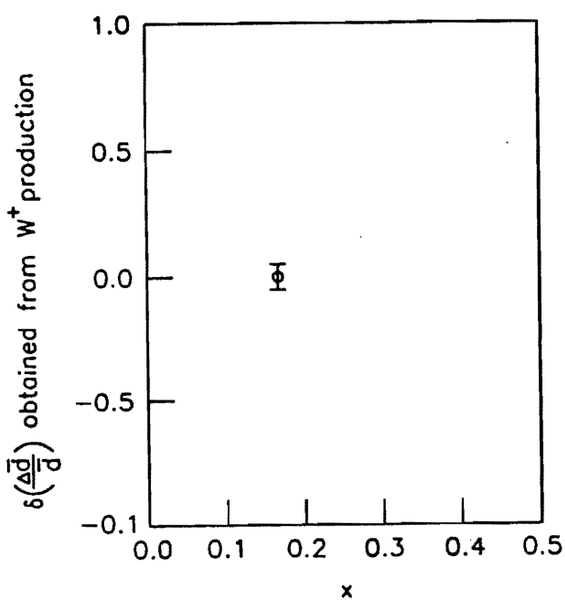

Figure 3

$\delta\left(\frac{\Delta\bar{d}}{\bar{d}}\right)$ obtained from

$pp \rightarrow W^+ + X$

ii). Parity-Conserving Asymmetry

For W^+,

$$A_{LL} \sim \frac{\Delta u(x_1)\,\Delta\bar{d}(x_2)}{u(x_1)\,\bar{d}(x_2)}.$$

A similar expression is for W^- production by permuting u and d.

4.1.7 Measurements of $h_1(x)$ (Quark Transversity Distribution in Polarized Proton)

A complete quark-parton model of the nucleon requires three quark distributions and quark spin density matrix is given as:

$$P(x) = 1/2\left[f_1(x) + g_1(x)\vec{s}_{//} \bullet \vec{\sigma} + h_1(x)\,\vec{s}_{\perp} \bullet \vec{\sigma}\right],$$

where f_1 (x) is related to the longitudinal momentum distribution of quarks in the nucleon, g_1 (x) is related to the helicity distribution in a polarized nucleon, and $h_1(x)$ is the fraction of transverse polarization of a proton carried by its quarks. The $h_1(x)$ can be determined by measuring the transverse spin correlation A_{TT} (A_{NN}) in Z° production.[4]

In terms of $h_1(x)$, A_{TT} (A_{NN}) is given as:

$$A_{TT} = \hat{a}_{TT}\,\frac{\sum_i \left(a_i^2 - b_i^2\right) h_{1_i}(x_1)\bar{h}_{1_i}(x_2)}{\sum_i \left(a_i^2 + b_i^2\right) f_{1_i}(x_1) f_{1_i}(x_2)},$$

where a_i and b_i are the vector and axial couplings of the Z° to the quark flavor i, $\hat{a}_{TT}$ is the partonic double-spin asymmetry, $\hat{a}_{TT} = 1$ at the vicinity of $\theta_{c.m.} = \pi/2$ and $\phi_{c.m} = 0$. The statistical error will be $\Delta A_{TT} = (1/P^2) \bullet 0.025$. At a first approximation $h_1 = g_1$, then $|A_{TT}/\hat{a}_{TT}| \sim |A_{LL}|$. This Z° production result generalizes the case of lepton-pair production[5] corresponding to $b_i = 0$ and $a_i = e_i$, the electric charge of q_i.

We now discuss several $h_1(x)$ measurements and examine their advantages and disadvantages. The $h_1(x)$ can also be determined by measuring the transverse spin correlation A_{TT} in jet-jet production. The $\hat{a}_{TT}$ for di-jet production is considerably smaller[6] (very fast fall when we leave the $\theta = 90°$ region) than for Z° production, but event rates are much larger. Furthermore, we measure h_1^2 in the jet-jet production while we determine $h_1 \bullet \bar{h}_1$ in Z° production. If $\bar{h}_1$ is close to zero, we can not measure h_1.

i) *Can We Find Z° in $Z \rightarrow$ Jet + Jet Decay?*

Branching ratio for $Z \rightarrow e^+e^-$ is 3.366 while for $Z \rightarrow$ jet + jet is 69.90. Construction efficiency of both cases were compared. Hadrons have a very wide spectrum causing a greater background. A lot of tricks have to be applied to suppress the background.

ii) *$pp \rightarrow$ Jet-Jet + X*

If one flavor is dominant, then $A_{TT} = \hat{a}_{TT}\ (h_1/q)^2$ and $\Delta A_{TT} = 2 \bullet \hat{a}_{TT}\ (h_1/q) \bullet \Delta(h_1/q)$. From jet-jet production we want $qq \rightarrow qq$, but jet-jet includes qq, qg, and gg depending on the range of p_T values. We also need to investigate the $q\bar{q}$ contribution, where the $\hat{a}_{TT}$ is much larger than that of qq.

By using CTEQTM structure function, the cross sections of qq, qg, and gg in $pp \rightarrow 2$ jets + X vs. p_T were calculated including the geometrical efficiency.[7]

We will see how well we can determine the values of (h_1/q). In this estimate, we choose a p_T region were S(qq)/BG (qg + gg) is 1/2 for $\sqrt{s}$ = 200 GeV and is 1/3 for $\sqrt{s}$ = 500 GeV as shown in Figs. 4 and 5.

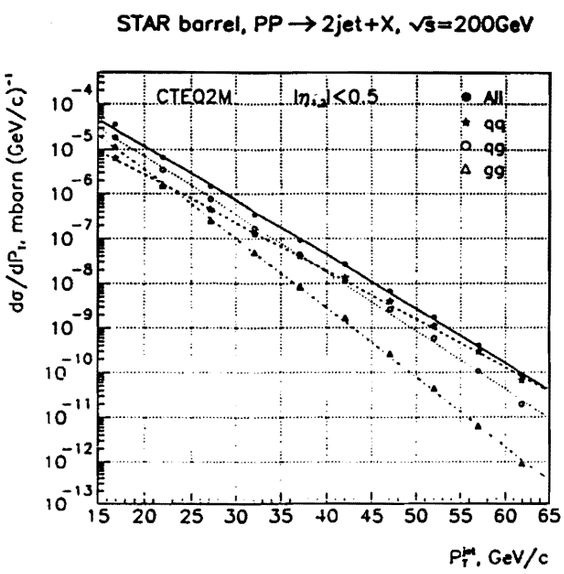

Figure 4

$pp \rightarrow 2$ jet + X vs. p_T at 200 GeV

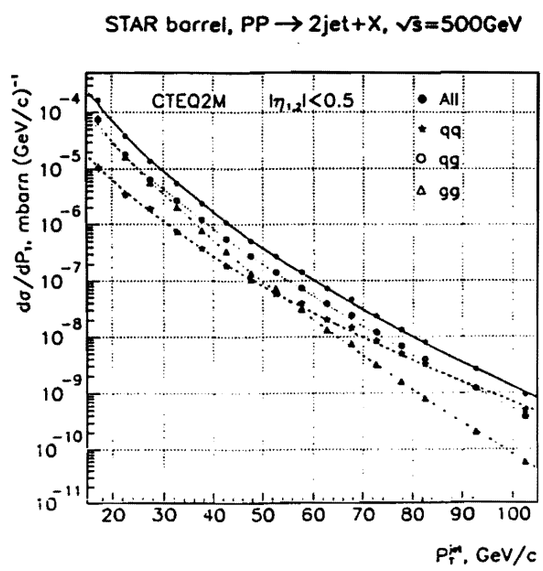

Figure 5

$pp \rightarrow 2$ jet + X vs. p_T at 500 GeV

We also need to remember that because of the transverse measurement, we loose a factor of two in ϕ coverage, and because of the limited useful θ region, mentioned above, we loose another factor of two.

For pp $\rightarrow$ jet-jet at 200 GeV, at $p_T > 25$ GeV/c where S(qq)/BG (qg + gg) = 1/2, we have 538,000 qq events. By considering ϕ and θ ($\hat{a}_{TT} \approx 0.05$) coverage, we have 135,000 useful events.

Then we have $\Delta A_{TT} = 2/\sqrt{135{,}000} = 2/370$. Because of S/B = 1/2 $\Delta A_{TT} = \sqrt{3} \bullet 2/370 = 0.01$. By assuming $(h_1/q) = 0.3$ (nonrelativistic case $(h_1/q) = g_1$) then $\Delta(h_1/q) = 0.01/[0.1 \bullet 0.3] = 0.3$. Thus, we will have $(h_1/q) = 0.3 \pm 0.3$ for $p_T > 25$ GeV/c (jet efficiency was not included).

For pp $\rightarrow$ jet-jet at 500 GeV, at > 45 GeV we have S(qq)/BG(qg + gg) = 1/3 and there are 526,000 qq events. Then useful events are 130,000 qq events. Then we have $\Delta A_{TT} = 2/\sqrt{130{,}000} = 0.006$. Because of Signal/BG = 1/3, $\Delta A_{TT} = 2 \bullet 0.006 = 0.012$, yielding $\Delta(h_1/q) = 0.012/[0.1 \bullet 0.3] = 0.4$. Thus, we will have $(h_1/q) = 0.3 \pm 0.4$ for $p_T > 45$ GeV/c (jet efficiency was not included).

iii) *$q\bar{q}$ Contribution*

The relative contributions are about 2% for $\sqrt{s} = 200$ GeV, and about 4% for 500 GeV. When one considers $\hat{a}_{TT} = 0.05$ for qq $\rightarrow$ jet-jet and $\hat{a}_{TT} = 1/\pi$ for $q\bar{q}$, it seems that the $q\bar{q}$ contribution is not negligible.

iv) *pp $\rightarrow Z^\circ + X$ at 500 GeV*

For simplicity, if one flavor is dominant then $A_{TT} = \hat{a}_{TT}\ (h_1/q)(\bar{h}_1/\bar{q})$, $(\Delta A_{TT})^2 = 2 \bullet (\hat{a}_{TT})^2 \bullet (h_1/q)^2\ (\Delta(\bar{h}_1/\bar{q}))^2$. By simply assuming $h_1/q = 0.3$ and $h_1/q = -0.3$, and $\hat{a}_{TT} = -1/\pi$ (X. Ji, Phys. Lett. B284 (1992) 137).

We have 1350 useful Z° events and then $\Delta A_{TT} = 2\sqrt{1350} = 0.05$, then $\Delta(h_1/q) = 0.05/(1.4 \bullet 0.1) = 0.3$. We will have $h_1/q = 0.3 \pm 0.3$.

(Note - actually we can not determine h_1/q in pp $\rightarrow Z^\circ + X$, but a simple comparison to pp $\rightarrow$ jet-jet was attempted.)

4.2 Measurements with Barrel, One Endcap and Shower Maximum Detector

An endcap calorimeter is to be placed inside the iron pole pieces. The endcap increases solid angle and acceptance and allows better measurements of the following reactions.

i) *Detecting the Direct-γ and the "Away-Side" Jet*

In order to measure $\Delta G(x)$, the gluon spin structure function, both the direct-γ and the "away-side" jet must be detected in coincidence so that the kinematics of the incoming parton can be calculated.

The Compton and annihilation subprocesses both involve $2 \rightarrow 2$ scatterings. The incoming partons are assumed to have fractions x_1 and x_2 are given in terms of pseudorapidity as:

$$x_1 \simeq \left(2p_T / \sqrt{s}\right) \left(e^{\eta_1} + e^{\eta_2}\right) / 2, x_2 \simeq \left(2p_T / \sqrt{s}\right) \left(e^{-\eta_1} + e^{-\eta_2}\right) / 2.$$

Figure 6 shows the x coverage for $x_T = 0.1$ as functions of the direct-γ and jet pseudorapidities. Figure 7 shows anticipated accuracy of $\Delta G/G$ determination.

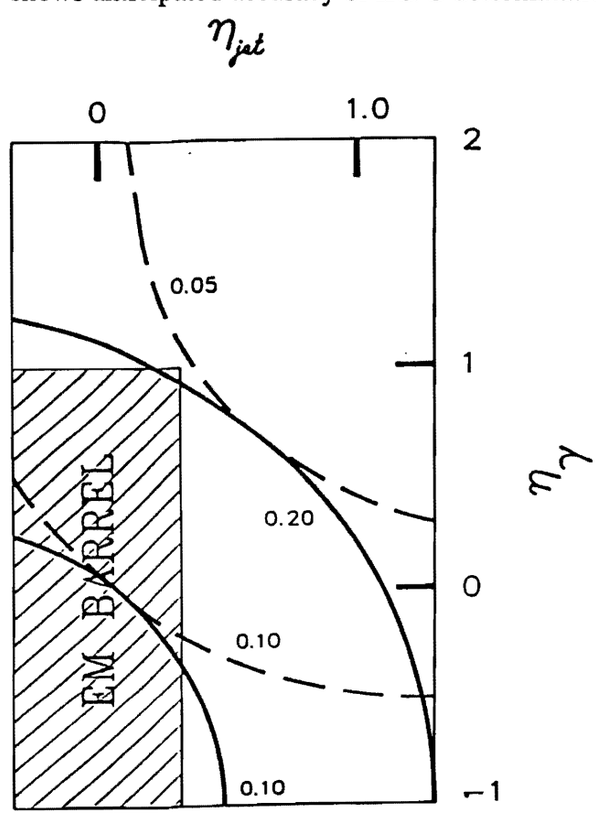

Figure 6 Plots of x_1 and x_2 as a function of the direct-γ and jet pseudorapidities. The solid lines represent contours for x_1 and the dashed lines are contours for x_2.

NAME | I D No. | M.S.
RETURN TO FERMILAB LIBRARY

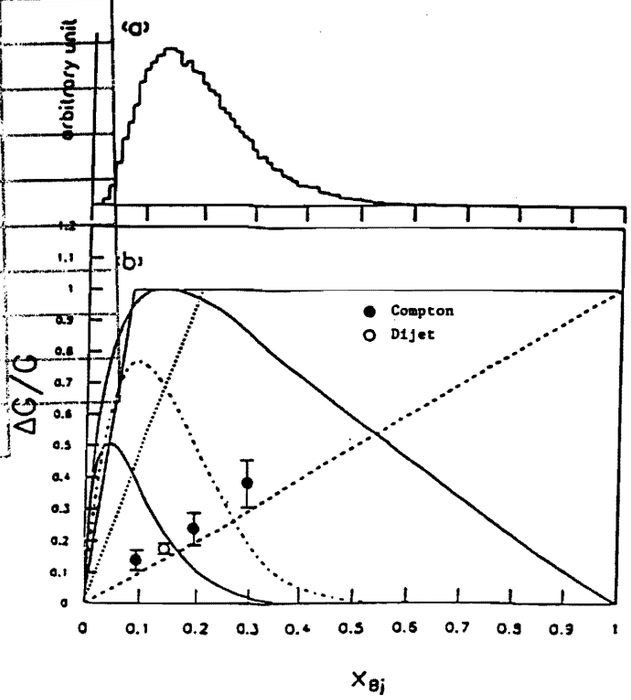

Figure 7 Measurement of ΔG/G vs. x.

ii) W's and Z Production at 500 GeV

We will have W^+ 74,000 events and W^- 22,000 events. For W's the detected electron (or positron) has $p_T > 20$ GeV/c. For Z° we will have 5,300 events and for Z at least one of the detected electrons have $p_T > 20$ GeV/c. In particular, many Z events are needed for a reasonable measurement of $h_1(x)$.

References

1. The Electromagnetic Calorimeter for the Solenoidal Tracker at RHIC, PUB-5380 (1993).
2. C. Bourrely and J. Soffer, *Phys. Lett.* B314 (1993) 132.
3. A. D. Martin, W. J. Sterling, and R. G. Roberts, Preprint RAL-92-021 (1992).
4. C. Bourrely and J. Soffer, *Nucl. Phys.* B423 (1994) 329.
5. J. Ralston and D. E. Soper, *Nucl. Phys.* B152 (1979) 109; J. L. Cortes, B. Pire, and J. P. Ralston, *Z. Phys.* C55 (1992) 409; R. Jaffe and X. Ji, *Phys. Rev. Lett.* 67 (1991) 552; R. Jaffee and X. Ji, *Nucl. Phys.* B375 (1992) 527; X. Ji, *Nucl. Phys.* B402 (1993) 217.
6. K. Hidaka, E. Monsay, and D. Sivers, *Phys. Rev.* D19 (1979) 1503; X. Artru and M. Mekhfi, *Z. Phys.* C45 (1990) 669; X. Ji, *Phys. Lett.* B284 (1992) 137.
7. Private communication, K. Shestermanov.